

A phenomenological view of Fermi-INTEGRAL gamma-ray Blazars, in the framework of leptonic SSC and EC scenario

Andrea Tramacere*

ISDC, Data Centre for Astrophysics Chemin d'Ecogia 16 CH-1290 Versoix Switzerland

E-mail: andrea.tramacere@unige.ch

Claudio Ricci & Roland Walter

ISDC, Data Centre for Astrophysics Chemin d'Ecogia 16 CH-1290 Versoix Switzerland

We propose a phenomenological approach that uses the spectral features of the rising part of the Inverse Compton emission of the blazars Spectral Energy Distribution, to derive the low-energy branch of the energy distribution of the emitting particles. We base our analysis on a leptonic, single-zone, homogeneous, Synchrotron Self-Compton, and External Compton scenario. Our analysis shows that it is possible to use the values of photon index (α_X) observed in *INTEGRAL* Flat Spectrum Radio Quasars (FSRQs) and intermediate/low-peaked BL Lacs (I/LBLs), and the photon index (α_γ) observed in *Fermi*-LAT high-peaked BL Lacs (HBLs), to constrain the low-energy cut-off (γ_{min}), and the low-energy photon index (s), of the emitting particles energy distribution. We found, in the case of FSRQs and I/LBL Lacs, that *INTEGRAL* data rule out a scenario with $\gamma_{min} \gg 1$. In the case of HBLs, Fermi data hints for a scenario with $\gamma_{min} \ll 10^4$, in agreement with previous analysis of the HBL Mrk 421, based on simultaneous X-ray-to-UV data. The predicted ranges for s , derived from observed data, are $\approx [1.6 - 2.4]$, and $\approx [1.2 - 2.8]$, respectively for HBLs, and FSRQs and I/LBLs. The similarity in the range of the predicted values of s , and the same trend of the position of the low-energy cut-off of the electron distribution, observed in FSRQs and BL Lacs, are interesting features, hinting for a common acceleration scenario acting in the two classes of objects.

*8th INTEGRAL Workshop The Restless Gamma-ray Universe September 27-30, 2010
Dublin Ireland*

*Speaker.

1. Introduction

Blazars are Active Galactic Nuclei (AGNs) characterized by a polarised and highly variable non-thermal continuum emission extending from radio to γ -rays. In the most accepted scenario, this radiation is produced within a relativistic jet that originates in the central engine and points close to our line of sight. Blazars come in two main flavours: BL Lac objects and Flat Spectrum Radio Quasars (FSRQs). The former type is characterised by featureless optical spectra and their SEDs are usually interpreted in the framework of pure synchrotron self Compton model (SSC) (Jones et al., 1974; Ghisellini & Maraschi, 1989). On the contrary, FSRQs display the prominent emission lines that are typical of QSOs, and are likely to have the inverse Compton (IC) component dominated by the external radiation Compton (EC) emission (Sikora et al., 1994; Dermer & Schlickeiser, 2002). BL Lac objects are often subdivided into three subclasses depending on their SEDs. This classification (Padovani & Giommi, 1995) uses the peak energy of the synchrotron emission, which reflects the maximum energy the particles can be accelerated in the jet, to classify BL Lacs into low energy, intermediate energy, and high energy synchrotron peak objects, respectively called LBL, IBL, and HBL. The broad band spectral energy distribution of Blazars depends strongly on the shape of the underlying emitting particle distribution. Although radiative processes are quite well understood, the acceleration processes are still not completely understood, and several possible mechanisms are likely to explain the observed phenomenology. This degeneracy is due to the lack of a complete constraining of the shape of the emitting particle distribution. In particular, it is often difficult to find direct observational signatures to constrain the low energy branch of the emitting particle distribution, namely the lowest energy of the emitting particle distribution (γ_{min}) and its spectral slope (s). We propose a phenomenological approach that uses the spectral features of the rising part of the IC component of blazars, to derive γ_{min} and s . In this regard, we selected the sample of FSRQs and I/LBLs already detected by *INTEGRAL* and *Fermi*-LAT, and the sample of HBLs detected by *Fermi*-LAT (Abdo et al., 2010). The *INTEGRAL* sample consists of all the blazars detected by *INTEGRAL* IBIS/ISGRI (Ubertini et al., 2003) during its first 8 years of operations. The *INTEGRAL* spectra were extracted in the 17–150 keV range from an all-sky mosaic, created using all the public science windows as of May 2010 (see for details Ricci et al. (2011)). We decide to study FSRQs and I/LBLs in the *INTEGRAL* hard-X-ray windows because, for these objects, the *INTEGRAL*/ISGRI instrument is sampling the rising part of the IC SED, at frequencies where are emitting low energy particles. This allows us to use these spectral features to investigate the low energy branch of the electron distribution. Since we are dealing with low-energy particles, these particle are not cooling dominated, introducing in our estimates a low cooling contamination to the accelerative signature. A parallel scenario applies if we investigate the rising part of the HBLs IC emission through the *Fermi*-LAT spectral window.

2. Phenomenological investigation of the low-energy branch of the electron distribution

Our analysis relies on the study of the dependence of the rising part of the IC emission on the low-energy branch of the electron distribution. Our goal is to derive γ_{min} and s from the photon index (α_X) observed by *INTEGRAL*/ISGRI (in the case of FSRQs and I/IBLs), and to derive the

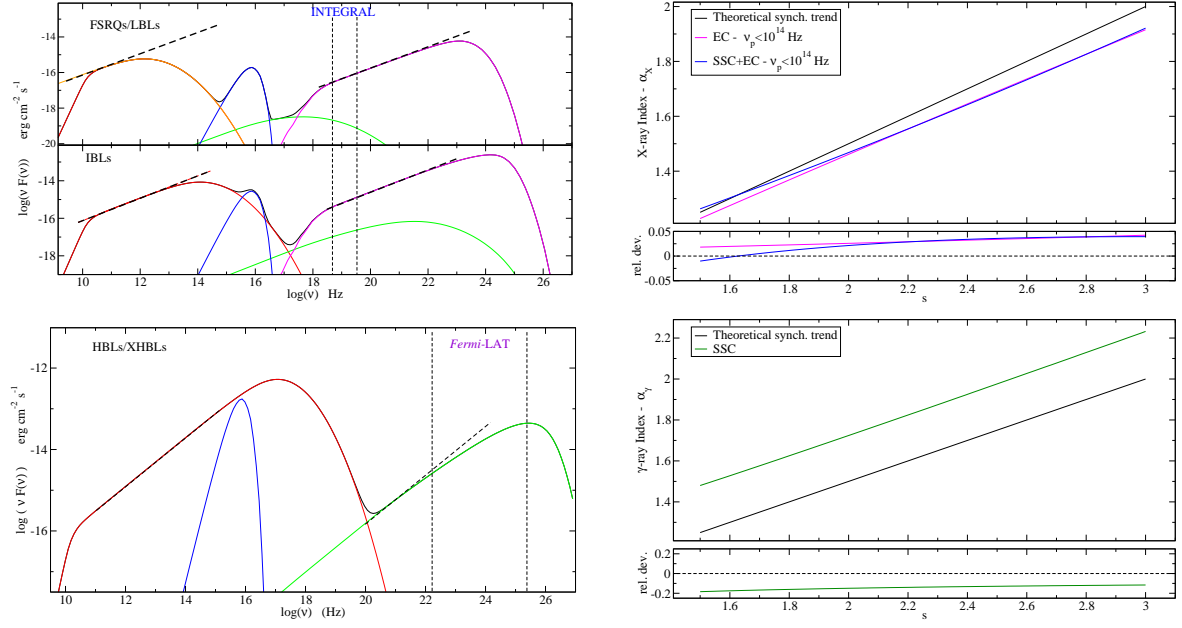


Figure 1: *Left panels:* typical SEDs for FSRQs/LBLs/IBLs (upper panel) and HBLs (panel b), the model shows: the synchrotron component (red line: with self-absorption, orange: without self-absorption), the SSC component (green line), the EC emission (purple line), the BBB emission (blue line), and the dashed black line represent the sum of all the components. The dashed thick oblique black line shows the approximate spectral slope. The vertical dashed lines represents the *INTEGRAL*/ISGRI window restricted to 17-150 keV, and the *Fermi-LAT* window restricted to 100 MeV 6- 100 GeV. *Right panels:* trend between α_X vs s (upper panel), and α_γ vs s (lower panel), with s ranging in [1.5-3.0], for SSC (green line), EC (purple line), and SSC+EC (blue line). The black thin line represents the theoretical expectation from standard synchrotron theory, the relative deviations of α_X , and α_γ w.r.t. synchrotron expectations are reported in the bottom panel.

same parameters by the observed values of α_γ in the *Fermi-LAT* spectral window (in the case of HBLs). To model the blazars SED, and to obtain trends among $s, \gamma_{min}, \alpha_X$, and α_γ we use an accurate numerical code (Tramacere et al., 2009), deriving trends by looping over the parameters of interest.

2.1 Linking s to α_X and α_γ

The left panels of Fig. 1 show by an oblique dashed black line that, both in the case of FSRQs and I/LBLs (top panel), and HBLs (bottom panel), the rising part of the synchrotron component, and the rising part of the IC emission, have similar spectral slopes. We stress, that in the case of FSRQs and LBLs, the synchrotron self-absorption (red line, upper left panel) usually hides the spectral portion linked to s (orange line, left upper panel), hence for this class of objects *INTEGRAL* data represent a unique tool to infer this parameter. According to the standard synchrotron theory (Rybicki & Lightman, 1979), the observed synchrotron photon index is linked to s by the well known relation: $\alpha \simeq (s - 1)/2 + 1$. By showing that the value of α_X and α_γ , observed in the IC emission, are close to the value of the photon index observed in the synchrotron spectrum range ruled by the spectral slope s , we demonstrate that we can use the α_γ , and α_X to derive s , that is our

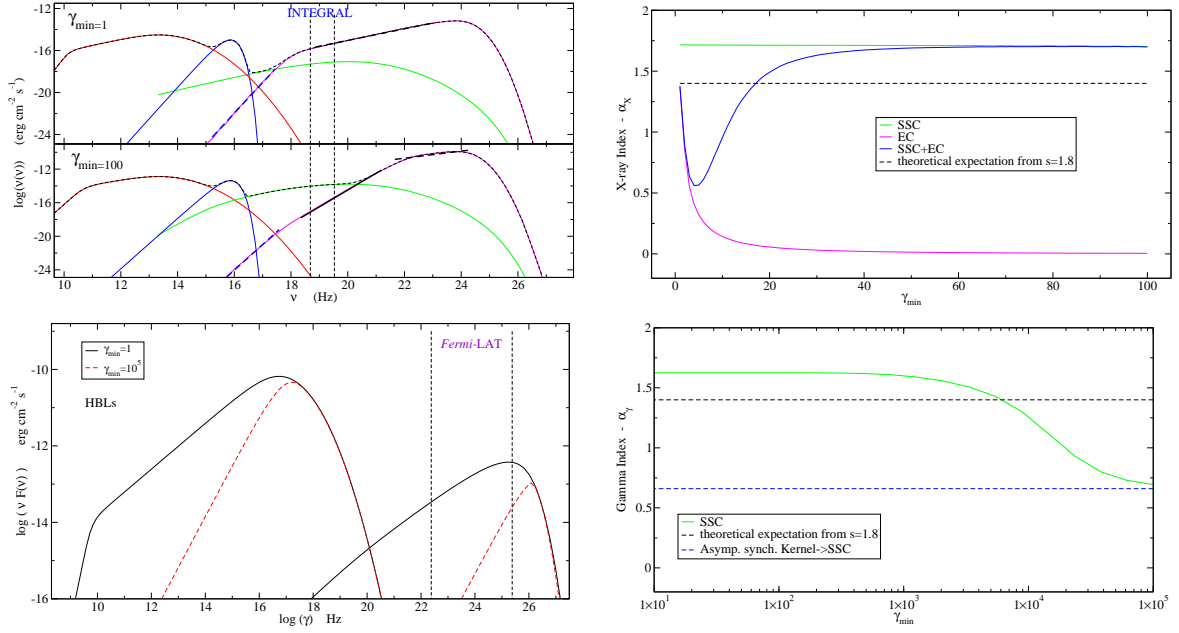


Figure 2: Left panels: Evolutions of the typical SEDs as a function of γ_{min} , same color code as in left panels of Fig. 1. Upper panel shows the case of FSRQs and I/LBLs for $\gamma_{min}=1$, and $\gamma_{min}=100$, lower panel shows the case of HBLs for $\gamma_{min}=1$, $\gamma_{min}=1e5$ (lower panel). Right panels: the trend between α_X and γ_{min} (upper panel, case of FSRQs and IBLs/LBLs), and α_γ vs. γ_{min} (case of HBLs), fixing $s=1.8$ in both cases.

goal. The right panels of Fig. 1 show the trend of α_X vs s (FSRQs, and I/LBLs, top panel), and α_γ vs s (HBLs, bottom panel). We obtained α_X and α_γ by fitting the numerically computed SEDs in the 17-150 keV band, for the case of *INTEGRAL*/ISGRI and in the 100 MeV - 100 GeV band, for the case of *Fermi*-LAT. We computed numerical SEDs with s ranging in [1.5-3.0]. In the case of FSRQs and I/LBLs (right top panel), both EC and EC+SSC values of α_X are close to the theoretical expectation from synchrotron theory (black line) within $\approx 5\%$. We note some deviation of the SSC+EC from the pure EC trend for $s < 2$. This is due to the larger contribution from the SSC component when s is harder. In the case of α_γ for HBLs, we get still a good correlation between s and α_γ , but s values are systematically softer compared to synchrotron theory prediction, within $\approx (15 - 20)\%$. We stress, that in the case of HBLs, a sampling of the rising part of the synchrotron component, is not easy, Indeed, it would require at least Optical and radio/mm data, and also the removing of the contamination from the galaxy contribution. *Fermi*-LAT data, hence gives values of s with a lower bias when compared to those coming from Optical and radio/mm data.

2.2 Linking γ_{min} to α_γ and α_X

To derive the value of γ_{min} we investigate the evolution of the shape of the rising part of the IC component as γ_{min} is increasing. For the classes of FSRQs and I/LBLs, we compare the two cases of $\gamma_{min}=1$ and $\gamma_{min}=100$ in the left upper panels of Fig. 2. For $\gamma_{min}=1$ the rising part of the EC component presents two branches, the one indicated by the dashed blue line has the same photon index of the Rayleigh-Jeans region of the external thermal photon field. This branch falls typically below the ISGRI spectral window. There is a second branch, whose photon index is determined

by the slope of the electron distribution (as discussed in the previous section) indicated by a black dotted line. This branch falls typically in the *INTEGRAL*/ISGRI spectral range. In the case of $\gamma_{min}=100$, it is evident that the *INTEGRAL* window is not anymore dominated by the electron power law index, on the contrary α_X approaches asymptotically the value of 0. In the right upper panel of Fig. 2 we show the trend of α_X vs s , obtained fitting our numerical SEDs. We plot the value of α_X as a function of γ_{min} , fixing $s = 1.8$. The expected values of α_X , for the case of $\gamma_{min}=100$ and for the EC and the EC+SSC cases, are significantly different from the prediction for the case $\gamma_{min}=1$, hence the *INTEGRAL* photon index offers a good signature to constrain the value of γ_{min} . We also stress, that the *INTEGRAL* window is quite far from the EC branch contaminated by the thermal external photon field, hence *INTEGRAL* data offer a better estimator for s compared to X-ray detector operating in the typical 0.2-10 keV band.

In the left lower panel of Fig. 2 we investigate the case of HBLs, by comparing the two scenarios of $\gamma_{min}=1$ and $\gamma_{min}=10^5$, both for the same value of $s = 1.8$. In both the cases ($\gamma_{min}=1$ and $\gamma_{min}=10^5$), we should observe in the power-law branch of the synchrotron and IC emission, the photon index determined by $s = 1.8$. Actually, we get this value only in the case of $\gamma_{min}=1$. This behavior has the following explanation. If we denote by $\nu_S(\gamma) \simeq 3.7 \times 10^6 B \gamma^2$ (Hz), the typical rest-frame energy emitted by a particle with a Lorentz factor of γ , interacting with a magnetic field of intensity B , and radiating synchrotron emission, we have that above $\nu_S(\gamma_{min})$, the emitted spectrum photon index will be determined by s , according to $\alpha \simeq (s - 1)/2 + 1$. Below $\nu_S(\gamma_{min})$, the synchrotron spectrum will be described by the asymptotic low-energy approximation of the single particle synchrotron emission, that is a power law with the photon index $\alpha \simeq -3/4$ (Rybicki & Lightman, 1979). In the right lower panel of Fig. 2, we plot the expected trend of α_γ vs γ_{min} , obtained by fitting the numerical SED in the *Fermi*-LAT spectral window, for the value of $s = 1.8$. For values of $\gamma_{min} \lesssim 10^4$, α_γ is close to the synchrotron expectation within $\simeq 15\%$. For values of γ_{min} above $\simeq 10^4$, it approaches the asymptotic low-energy approximation of the single particle synchrotron emission. This analysis, shows clearly, that the spectral shape in the *Fermi*-LAT window can be used as a good estimator of the value of γ_{min} in the case of HBLs.

3. MonteCarlo approach and Comparison with observed statistics

To compare our predicted trends with the observed data we use a MonteCarlo (MC) approach. Specifically, we generate both the SSC and EC numerical computation of the SEDs, extracting the input parameters of the models from a random distribution. This allows us to cover a larger volume of the parameter space, and to investigate how the trends, discussed above, changes when several parameters are changing simultaneously. In the case of FSRQs and I/LBLs, we make two MC runs, randomizing all the models parameters, and fixing $\gamma_{min}=1$ and $\gamma_{min}=100$ respectively. The corresponding results are summarized in the left panel of Fig. 3. The observed α_X distribution of *INTEGRAL* FSRQs and I/LBLs (red line) is clearly compatible with the case of $\gamma_{min}=1$, (blue line) and rules out the case of $\gamma_{min}=100$, both in the EC dominated scenario (green line) and in the SSC+EC case (green dashed line). Moreover, from the range of the observed $\alpha_X \simeq [1.0 - 1.8]$ we estimate a corresponding range for $s \simeq [1.2-2.8]$. To study Fermi HBLs, we make two MC runs, fixing $\gamma_{min}=1$, and $\gamma_{min}=10^4$, respectively. The results are summarized in the right panel of Fig. 3. Also in this case, we are able to rule out the scenario with a large value of γ_{min} ($\gamma_{min}=10^4$,

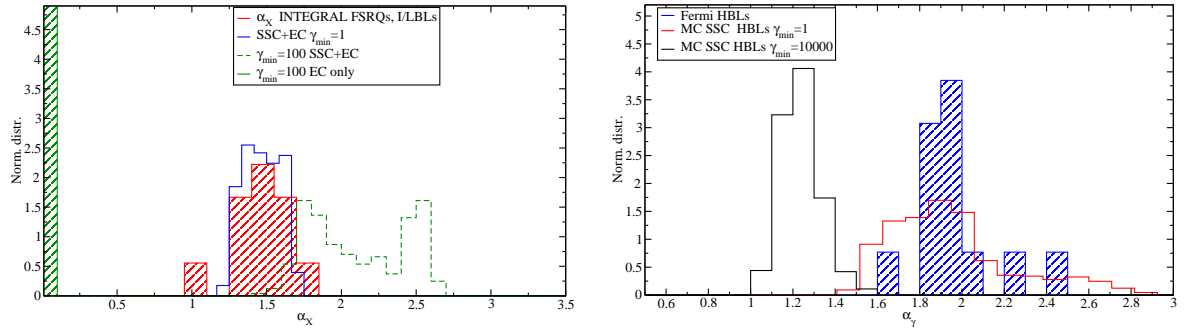


Figure 3: Histograms for MC runs for the FSRQs and I/LBLs compared to *INTEGRAL* observed α_X statistics (left panel), and for the HBLs compared to *Fermi-LAT* observed α_γ statistics (right panel).

black line). The case of $\gamma_{min}=1$ shows a better matching with the observed Fermi values of α_γ , and shows also the same drop in the histogram around the value of $\alpha_\gamma \simeq 2$. The observed range of $\alpha_\gamma \simeq [1.5 - 2.5]$ returns a range for $s \simeq [2.0-3.0]$, taking into account, that in the case of the SSC scenario, as shown in Sect. 2.1, there is systematic softening of s of about a 20%, the fiducial range for s should be $\simeq [1.6 - 2.4]$

4. Conclusions

We showed that is possible to use the values of α_X observed in *INTEGRAL* FSRQs and I/LBLs, and α_γ observed in Fermi HBLs, to constrain γ_{min} and s . According to our analysis, in the case of FSRQs and I/LBLs, *INTEGRAL* data rule out a scenario with $\gamma_{min} \gg 1$. In the case of HBLs, Fermi data hints for a scenario with $\gamma_{min} \ll 10^4$, in agreement with previous analysis of the HBL object Mrk 421 based on simultaneous X-ray-to-UV data (Tramacere et al., 2009). The predicted range for s , derived from observed data, are $\simeq [1.6 - 2.4]$, and $\simeq [1.2 - 2.8]$, respectively for HBLs, and FSRQs and I/LBLs. The similarity in the range of the predicted values of s , and the same trend of the position of the low-energy cut-off of the electron distribution, observed in FSRQs and BL Lacs, are interesting features, hinting for a common acceleration scenario acting in the two classes of objects.

References

- Abdo, A. A., Ackermann, M., Ajello, M., et al. 2010, *The Astrophysical Journal*, 715, 429
 Dermer, C. D. & Schlickeiser, R. 2002, *ApJ*, 575, 667
 Ghisellini, G. & Maraschi, L. 1989, *ApJ*, 340, 181
 Jones, T. W., O'dell, S. L., & Stein, W. A. 1974, *ApJ*, 188, 353
 Padovani, P. & Giommi, P. 1995, *MNRAS*, 277, 1477
 Ricci, C., Walter, R., Courvoisier, T. J.-L., Paltani, S. 2011, *A&A* in press, arXiv:1104.3676
 Rybicki, G. B. & Lightman, A. P. 1979, *Radiative processes in astrophysics* (New York, Wiley-Interscience, 1979. 393 p.)
 Sikora, M., Begelman, M. C., & Rees, M. J. 1994, *ApJ*, 421, 153
 Sikora, M., Blazejowski, M., Moderski, R., & Madejski, G. M. 2002, *ApJ*, 577, 78
 Tramacere, A., Giommi, P., Perri, M., Verrecchia, F., & Tosti, G. 2009, *A&A*, 501, 879
 Ubertini, P., Lebrun, F., Di Cocco, G., 2003, *A&A*, 411, 131